

## Antiferromagnetic resonance in $\text{Bi}_2\text{CuO}_4$

L. E. Svistov,<sup>\*</sup> V. A. Chubarenko, A. Ya. Shapiro, and A. V. Zaleskiĭ

*A. V. Shubnikov Institute of Crystallography, Russian Academy of Sciences, 177333 Moscow, Russia*

G. A. Petrakovskii

*L. V. Kirenskii Institute of Physics, Siberian Department of Russian Academy of Sciences, 660036 Krasnoyarsk, Russia*

(Submitted 10 November 1997)

Zh. Éksp. Teor. Fiz. **113**, 2244–2255 (June 1998)

Magnetic resonance of the low-frequency spin-wave branch in the  $\text{Bi}_2\text{CuO}_4$  antiferromagnet with an easy-plane anisotropy has been studied. Angular, frequency, and temperature dependences of the position and width of the antiferromagnetic resonance (AFMR) line have been measured. Our measurements combined with earlier data [H. Ohta, K. Yoshida, T. Matsuya, T. Nanba, M. Motokawa, K. Yamada, Y. Endon, and S. Hosoya, *J. Phys. Soc. Jpn.* **61**, 2921 (1992); E. W. Ong, G. H. Kwei, R. A. Robinson, B. L. Ramakrishna, and R. B. von Dreele, *Phys. Rev. B* **42**, 4255 (1990)] have allowed us to determine anisotropy constants of this material and to account for the unusual character of its static susceptibility anisotropy. The AFMR line shifts to the high-field side and broadens in a temperature range of 10–15 K, and the cause of this has remained unclear. In the low-temperature range the line shows a hysteresis corresponding to a static field magnitude several times as large as the spin-flop field. The position and width of the AFMR line depend sensitively on the sample preparation technique. © 1998 *American Institute of Physics*. [S1063-7761(98)02406-8]

### 1. INTRODUCTION

Study of materials containing ions of variable valence is one of rapidly developing branches of modern physics. They attract researchers' attention primarily in connection with the discoveries of high-temperature superconductivity and giant magnetoresistance in such materials.

One representative of this class is  $\text{Bi}_2\text{CuO}_4$ , whose structure belongs to the space group  $P4/ncc$ .<sup>2–4</sup> The magnetic moment of the  $\text{Cu}^{2+}$  cation is due to a single uncompensated electron in the  $d$ -shell. Neutron diffraction studies<sup>2,4–6</sup> of  $\text{Bi}_2\text{CuO}_4$  indicate the presence of three-dimensional magnetic ordering at temperatures below  $T_N \approx 42$  K.

The unit cell of  $\text{Bi}_2\text{CuO}_4$  contains four copper ions. In the conventional notation,<sup>4</sup> the positions of these ions in the lattice are as follows: Cu(1),  $(1/4, 1/4, z)$ ; Cu(2),  $(1/4, 1/4, z + 1/2)$ ; Cu(3),  $(3/4, 3/4, 1/2 - z)$ ; Cu(4),  $(3/4, 3/4, -z)$ . The parameter  $z$  is the shift of the parallelepipeds formed by Cu(1) and Cu(2) ions with respect to those of Cu(3) and Cu(4) ions along the  $C^{(4)}$  axis. The value of  $z$  equals 0.076 of the lattice constant  $c$ .<sup>4</sup> The chains of Cu(1), Cu(2) and Cu(3), Cu(4) ions form two magnetic sublattices in the antiferromagnetically ordered state of  $\text{Bi}_2\text{CuO}_4$ . The magnetic anisotropy for  $\text{Cu}^{2+}$  ions is determined by the anisotropic exchange, since a one-ion anisotropy due to the electric crystal field does not affect ions with spin 1/2. The exchange anisotropy aligns the magnetic moments of the sublattices within the plane perpendicular to the four-fold axis.<sup>6,7</sup> In the absence of magnetic field, the antiferromagnetic vector is directed along a diagonal of the  $(a, b)$  square in the easy

plane.<sup>8</sup> The effective magnetic moment of the  $\text{Cu}^{2+}$  ion in antiferromagnetic  $\text{Bi}_2\text{CuO}_4$  at 4.2 K is  $0.65 - 0.85 \mu_B$ .<sup>6,7</sup>

The electron spin resonance in the magnetically ordered phase ( $T < T_N$ ) was studied in the submillimeter wave region.<sup>1</sup> From these measurements, the energy gap separating the exchange (high-frequency) branch of the magnon spectrum was derived. The antiferromagnetic resonance of the lower branch of the magnon spectrum in  $\text{Bi}_2\text{CuO}_4$  single crystals grown from a melt was studied by Pankrats et al.<sup>8</sup> The frequency and angular dependences of the antiferromagnetic resonance field in the microwave and submillimeter wave bands were in good agreement with the magnetic structure of  $\text{Bi}_2\text{CuO}_4$  determined previously.<sup>6,7</sup>

The static magnetic characteristics of samples depend sensitively on their preparation technique. Crystals grown by the hydrothermal technique<sup>9</sup> have in the ordered state a small ferromagnetic moment  $m$  in the basal plane of less than one percent of the nominal  $\text{Cu}^{2+}$  magnetic moment, which drops as the static magnetic field grows and vanishes for  $H > 30$  kOe ( $T = 4.2$  K). Samples grown from a melt do not manifest a weak ferromagnetism.<sup>5,6</sup> In the range of strong static fields, the susceptibilities of both types of samples are equal. The small ferromagnetic moment in samples made by the hydrothermal method was attributed to the Dzyaloshinskii–Moria interaction.<sup>9</sup>

In the present work, we have studied the microwave electron spin resonance of  $\text{Bi}_2\text{CuO}_4$  single crystals of both types in the temperature range below  $T_N$ , and also in samples annealed after growth in an oxygen–helium atmosphere.

## 2. SAMPLES AND EXPERIMENTAL TECHNIQUES

We have studied  $\text{Bi}_2\text{CuO}_4$  samples grown both by the flux method and hydrothermal technique.<sup>10,11,13</sup>

The samples were tested by x-ray diffraction and x-ray microanalyzer. x-ray diffraction measurements using a D/max-3C microdiffractometer produced by Rigaku demonstrated identical crystal structures of samples prepared by the two techniques. Nonetheless, the quantitative analysis of the samples performed on a JXA-8600 electron microscope combined with an x-ray analyzer produced by JEOL, in which we used the ZAF-correction program and reference samples of copper and bismuth (the oxygen content was determined by subtraction) revealed differences between compositions of crystals made by the two different methods. Samples grown from a melt had the composition  $\text{Bi}_{1.9}\text{CuO}_{3.87}$ , whereas samples prepared by the hydrothermal technique had the formula  $\text{Bi}_{2.05}\text{CuO}_{3.84}$ .

The comparison between the formulas of crystals grown by different techniques indicates that the degree of oxidation of cations in crystals grown from the hydrothermal solution is slightly lower than in samples grown from a melt. This difference may be caused by the fact that it is difficult to create a high oxidation potential in an autoclave, therefore hydrothermal crystals are deficient in oxygen, and a small quantity of nonmagnetic  $\text{Cu}^+$  cations is present.

Experiments were performed on both as-grown crystals and samples annealed after growth in an atmosphere of oxygen or nitrogen. The annealing was performed at 600°C for 30 h. Note that the annealing in oxygen and nitrogen did not affect the positions and widths of AFMR lines in samples grown from a melt, but radically changed magnetic properties of samples made by the hydrothermal technique.

Typical dimensions of  $\text{Bi}_2\text{CuO}_4$  samples grown from a melt and hydrothermally were  $2 \times 2 \times 0.5$  and  $1 \times 1 \times 0.1$  mm<sup>3</sup>, respectively.

The electron spin resonance was measured on a transmission microwave spectrometer. A sample was placed in a rectangular cavity whose resonant modes were in the frequency band of 23–78 GHz. The device was designed to allow sample rotation during an experiment. A magnetic field of 0 to 40 kOe was produced by a superconducting solenoid. The cell with a sample was in a vacuum jacket, so that we could perform our measurements in a temperature range of 1.2 to 110 K. Measurements at a frequency of 9.3 GHz were performed on a commercial ESR spectrometer produced by Bruker.

## 3. EXPERIMENTAL RESULTS

### 3.1. Measurements of samples grown from melt solution

Figure 1 shows traces of microwave power transmitted through the cavity versus magnetic field at various temperatures. In the temperature range close to  $T_N$ , the ESR line is considerably broadened, and a new line forms at a magnetic field slightly higher than that of ESR. In the low-temperature range,  $T < 12$  K, the absorption line shape depends on the field scan direction. The solid curves in Fig. 1 were recorded in an increasing magnetic field, and the dashed curves in a

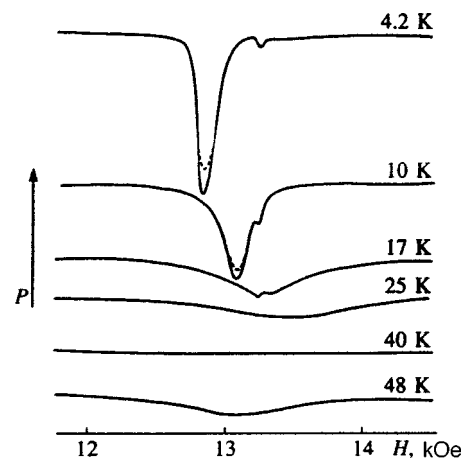


FIG. 1. Typical curves of microwave power transmitted through the cavity loaded with a  $\text{Bi}_2\text{CuO}_4$  sample grown from a melt versus magnetic field at several temperatures. The narrow resonance line whose position is independent of the temperature is due to a DPPH sample, which is used as a reference for measuring the applied static magnetic field. The solid curves were recorded when the field was scanned in the upward direction, the dashed lines correspond to decreasing magnetic field;  $\nu = 36$  GHz,  $H \parallel [110]$ .

decreasing field. The hysteresis behavior is more pronounced at lower magnetic fields, corresponding to lower resonant frequencies.

The position of the absorption line is strongly anisotropic. Measurements of angular dependence performed at different microwave frequencies and temperature have demonstrated that resonance conditions are determined by the static field projection on the plane perpendicular to the four-fold symmetry axis. When the static field was rotated in the basal plane, the line shift was well described by the function  $A \cos(4\varphi)$ . The resonant field had maxima when its direction coincided with the  $a$ - or  $b$ -axis.

The resonant field versus frequency is close to a linear function. The absorption peak is close to the ESR position of a paramagnet with  $g$ -factor  $g = 2$ . Note that resonant fields measured in earlier experiments with the same configuration<sup>1,8,12,14</sup> were also close to a straight line of the same slope. Figure 2 shows resonant fields of samples with respect to the resonant field of diphenylpicrylhydrazyl (DPPH), which was used as a reference ( $g = 2$  for DPPH). It is clear that the curve of the frequency dependence is steeper than that of the free radical at 25 K, whereas at lower temperatures it has a gentler slope.

The temperature dependence of the resonant field at a microwave frequency of 36 GHz is plotted in Fig. 3. Experiments have been performed with two orientations of the static field in the basal plane,  $\varphi = 0^\circ$  and  $45^\circ$ . The resonant field shifts to higher values in the temperature range of 10–15 K.

As was noted above, experiments have been performed on both as-grown samples and crystals annealed in the atmosphere of oxygen or nitrogen. Within the experimental uncertainty, the annealing has no effect on the resonances in  $\text{Bi}_2\text{CuO}_4$  crystals grown from a melt. The microanalysis of chemical composition also has not revealed any changes after annealing.

Figure 4 shows the AFMR line width as a function of

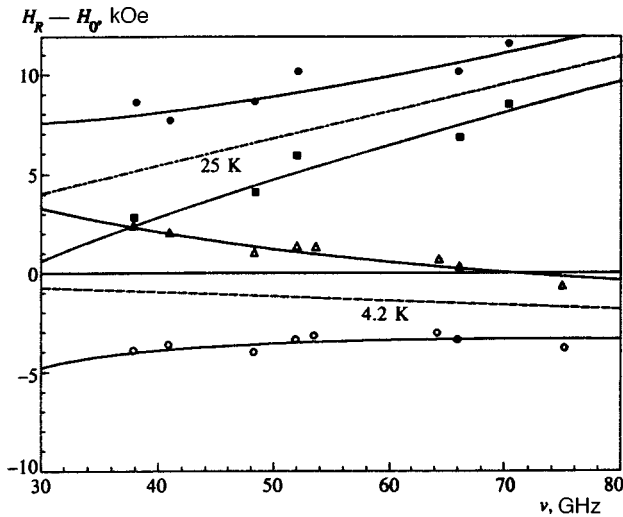


FIG. 2. AFMR field  $H_R$  measured with respect to the ESR field  $H_0$  for DPPH as a function of microwave frequency. Open symbols correspond to temperature  $T=4.2$  K, filled symbols to  $T=23$  K; filled squares and open circles correspond to  $H\parallel[110]$ , and filled circles and triangles to  $H\parallel[100]$ . The samples were grown from a melt. The solid lines are calculations of the AFMR field as a function of frequency by Eq. (2) with parameters  $H_A^{(4)}H_E=10$  and  $6.8$  kOe $^2$  and  $a/A=-0.02$  and  $-0.1$  at temperatures  $T=4.2$  and  $23$  K, respectively. The dashed and dash-dotted lines show calculations at  $\varphi=22.5^\circ$ , when the gap in the spectrum due to anisotropy in the plane perpendicular to the four-fold axis vanishes.

temperature for two nonannealed samples. One can see that the temperature-dependent parts of the AFMR line width are similar. The part of the line width independent of temperature is, most probably, due to an inhomogeneous line broadening and depends sensitively on the sample quality. The most plausible factor leading to the inhomogeneous broadening is variation in the alignment of the  $C^2$  axis over the crystal volume. No correlation between the line width and annealing conditions has been detected.

Recordings of the derivative of the absorbed microwave power with respect to magnetic field (at  $\nu=9.3$  GHz) as a function of the field are plotted in Fig. 5. Absorption lines recorded for both scanning directions have a rich fine structure, which manifests in the low-temperature range ( $T<15$  K). This fine structure is well reproducible. The fine structure is seen in the range of magnetic field below the antiferromagnetic resonance at all static field orientations in the basal plane.

### 3.2. Discussion

The changes in the resonant absorption with temperature (Fig. 1) and the strong dependence of the resonant field  $H_R$  on the static field orientation provide strong evidence in favor of an antiferromagnetic resonance in  $\text{Bi}_2\text{CuO}_4$ . Another argument in favor of the interpretation of the resonant absorption in terms of uniform precession of the magnetic moment is the fine structure in absorption spectra in the field range below the main resonance (Fig. 5). In all probability, the recorded fine structure is due to spin-wave resonances in  $\text{Bi}_2\text{CuO}_4$ . The presence of resonances corresponding to large wave numbers allows us to rule out an interpretation ascribing the absorption line to impurities.

The presence of the gapless branch in the spectrum of magnetic excitations is in accordance with submillimeter wave and microwave measurements,<sup>1,8</sup> and with neutron diffraction experiments,<sup>7</sup> but contradicts other neutronographic measurements.<sup>12</sup>

All resonance properties of  $\text{Bi}_2\text{CuO}_4$  can be easily described considering it as a two-sublattice antiferromagnet with an easy-plane magnetic anisotropy. A phenomenological theory of the antiferromagnetic resonance taking into account an easy-plane anisotropy was given by Turov.<sup>13</sup> The energy density of such an antiferromagnet is expressed as<sup>13</sup>

$$\mathcal{F}_m = A/2m^2 + a/2 m_z^2 + b/2 l_z^2 + f/2 l_x^2 l_y^2 - 2M_0 \mathbf{m}\mathbf{H}. \quad (1)$$

Here  $M_0$  is the saturation magnetization of one sublattice,  $\mathbf{l}$  and  $\mathbf{m}$  are the normalized vectors of antiferromagnetism and magnetization ( $m^2 + l^2 = 1$ ,  $\mathbf{m}\cdot\mathbf{l} = 0$ ). The first term on the right-hand side is the exchange energy, the second and third are responsible for the crystallographic magnetic anisotropy of a uniaxial crystal (in the case of an easy-plane anisotropy  $b>0$ ). The fourth-order term takes into account the anisotropy in the basal plane perpendicular to the  $[001]$  axis. The last term describes the magnetic energy due to applied magnetic field.

The two AFMR frequencies corresponding to the acoustic and optic magnon branches are given by

$$\omega_1 = \gamma[H^2(1 + a/A) - H_E H_A^{(4)} \cos(4\varphi)]^{1/2}, \quad (2)$$

$$\omega_2 = \gamma[H_E H_A]^{1/2}[1 - H^2/H_E^2]^{1/2}, \quad (3)$$

where  $\gamma = g_\perp \mu_B / \hbar = 18.15 \times 10^9 \text{ s}^{-1} \text{ kOe}^{-1}$  is the gyromagnetic ratio (according to Ref. 1  $g_\perp = 2.04$ ),  $H$  is the static magnetic field,  $H_E = A/2M_0$ ,  $H_A = b/2M_0$ , and  $H_A^{(4)} = (\gamma/2M_0)f$ . From the static susceptibility measured by Ohta *et al.*<sup>1</sup> for  $H \perp C^{(4)}$ , we derive  $H_E = 2M_0/\chi_{\perp c} = 2000$  kOe;  $H_A = 12$  kOe can be derived from the width of the gap separating the high-frequency AFMR branch.<sup>1</sup> From our measurements, we derive  $H_A^{(4)}$  and the ratio  $a/A$ . The solid line in Fig. 4 shows calculations of the frequency dependence of the AFMR field by Eq. (2) with  $H_E H_A^{(4)} = 10$  and  $6.8$  kOe $^2$  and  $a/A = -0.02$  and  $-0.1$  at temperatures  $T=4.2$  and  $23$  K, respectively. The curves of  $H_E H_A^{(4)}$  and  $a/A$  versus temperature are plotted in Fig. 3. The minus sign in front of  $a$  indicates the easy-axis anisotropy for the ferromagnetic vector  $\mathbf{m}$ , whereas the antiferromagnetic vector  $\mathbf{l}$  has an easy-plane anisotropy ( $b>0$ ). Given  $a/A$ , one can determine the ratio between the static susceptibilities  $\chi_\perp/\chi_\parallel = 1 + a/A$ .<sup>13</sup> The subscripts indicate the magnetic field orientation with respect to the four-fold axis  $C^{(4)}$ . It is clear that, given the negative  $a$  for  $\text{Bi}_2\text{CuO}_4$ ,  $\chi_\perp$  should be about 10% smaller than  $\chi_\parallel$  at  $T=20$  K, which is in reasonable agreement with static magnetic measurements.<sup>1,6</sup> It is remarkable that the temperature dependence of the anisotropy constant  $a$  (Fig. 3) is strong in the temperature range of 10–20 K, which is far from  $T_N$ . The AFMR line also broadens considerably in this temperature interval (Fig. 4). All these effects may be related to a structural transition in  $\text{Bi}_2\text{CuO}_4$ , because the unit cell volume also increases abruptly in this region.<sup>4</sup>

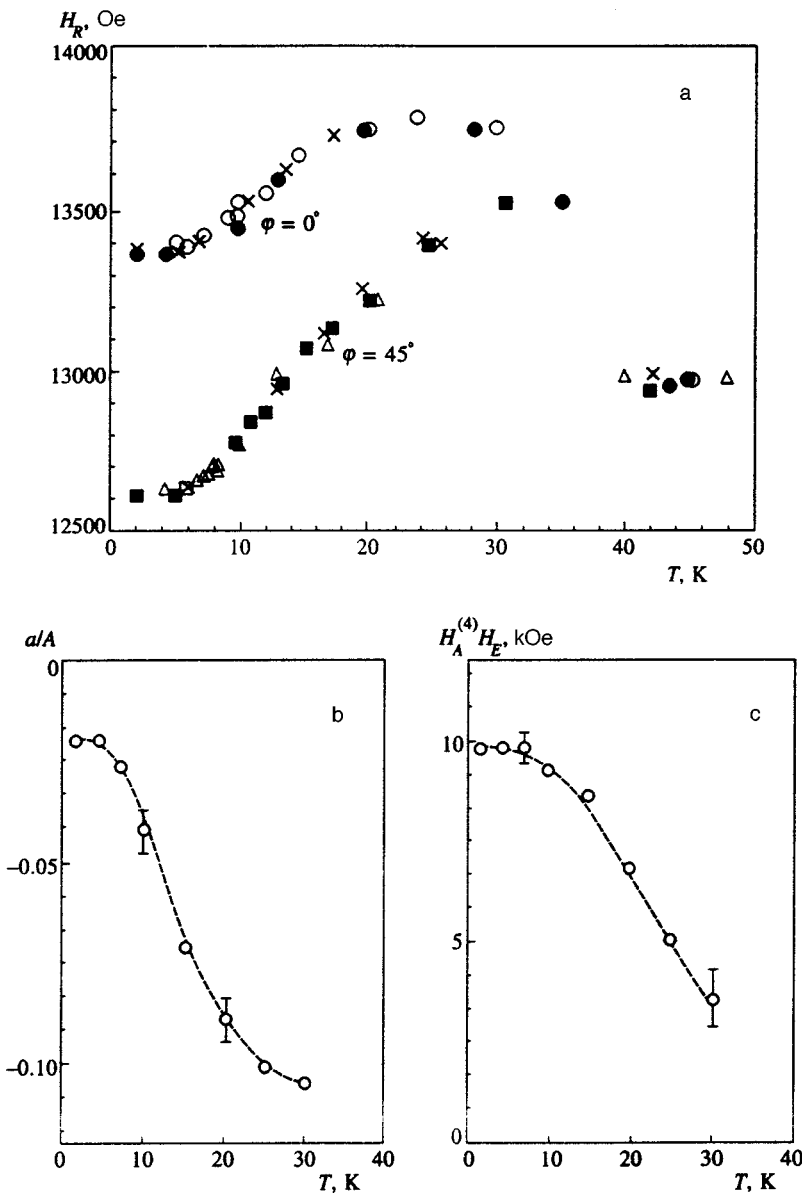


FIG. 3. (a) Resonant field versus temperature at microwave frequency  $\nu=36$  GHz. Measurements were performed for two orientations of the static field in the basal plane,  $\phi = 0$  and  $45^\circ$ . Different symbols show measurements of samples annealed in oxygen or nitrogen, and as-grown samples. Within the experimental uncertainty, curves of  $H_R(T)$  for all samples are identical. The samples were grown from a melt. (b) and (c) Temperature dependences of  $a/A$  and  $H_A^{(4)}H_E$  derived from measurements plotted in Fig. 3a.

In addition to the step on the curve of the AFMR line width versus temperature in the range of 10–15 K (Fig. 4), the width also grows rapidly as the temperature approaches the Néel temperature. This temperature-dependent part of the line width is largely due to the process of three-magnon relaxation. The solid curve in this graph shows calculations of the AFMR line width caused by the above mentioned relaxation process using the equation given in Ref. 15 and parameters of  $\text{Bi}_2\text{CuO}_4$  given in this section.

The hysteretic behavior of the absorption line up to fields several times larger than spin-flop fields indicates the presence of a highly developed system of antiferromagnetic domains. Unlike the case of a ferromagnet, antiferromagnetic domains are equivalent in energy terms in fields higher than the spin-flop field, so even a slight pinning makes a domain wall stable up to the high fields. It is probable that the shift of the resonance field, step-like growth of the line width, hysteretic behavior of the absorption line, and the abrupt change in the cell volume in the temperature range of 10–15 K are caused by a sharp decrease in the mobility of domain

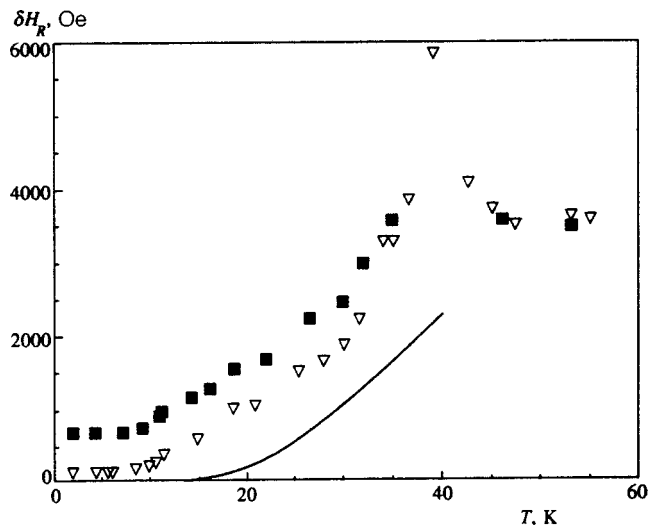


FIG. 4. AFMR line widths versus temperature at  $\nu=36$  GHz. Filled squares and triangles show measurements of two different as-grown samples. The solid curve shows calculations of line widths due to three-magnon relaxation based on formulas of Ref. 15. The samples were grown from a melt.

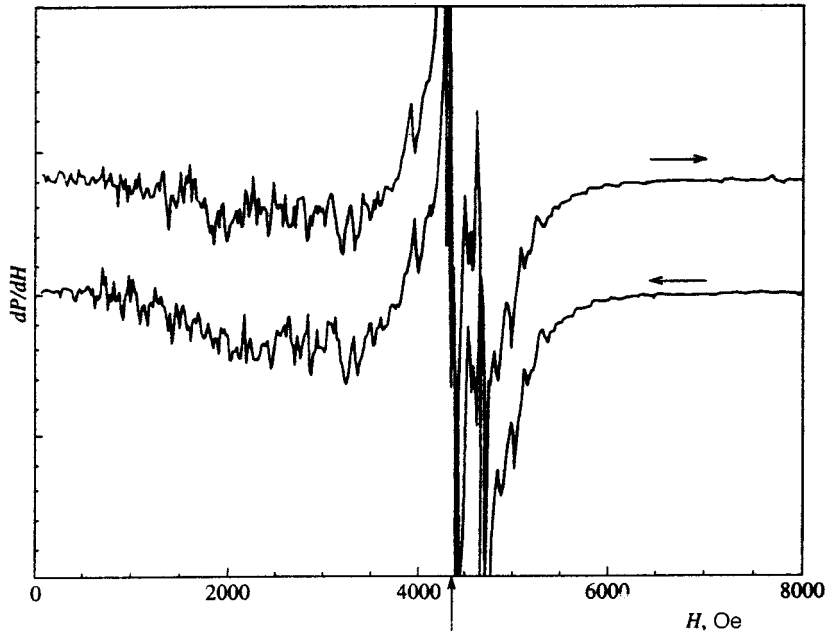


FIG. 5. Measurements of the derivative of the microwave power absorbed by the sample with respect to magnetic field as a function of applied magnetic field.  $\nu=9.3$  GHz,  $T=10$  K,  $\varphi=0^\circ$ . The arrow indicates the AFMR position calculated by Eq. (2) with the parameters corresponding to the given temperature. The lower graph shows curves on the extended magnetic field scale.



walls. Information about the nature of antiferromagnetic domains in  $\text{Bi}_2\text{CuO}_4$  may be derived from measurements of nuclear magnetic resonance and magneto-acoustic experiments.

**3.3. Measurements of samples grown by the hydrothermal technique and discussion**

In experiments with samples obtained by the hydrothermal technique, we have detected two lines of resonance absorption. Typical curves are given in Fig. 6. The field of resonance  $R1$  strongly depends on the direction of the static

field  $H$ , whereas the position of resonance  $R2$  is independent of its orientation. As in the case of samples grown from a melt, the conditions of resonance  $R1$  are controlled by the static field projection on the plane perpendicular to the four-fold axis. The position of the low-field resonance  $R1$  strongly depends on temperature (Fig. 7). At the same time,

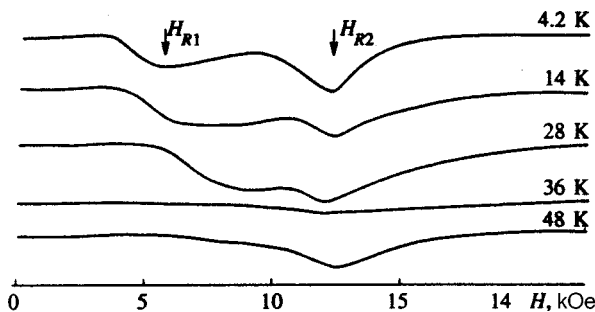


FIG. 6. Typical curves of microwave power transmitted through the cavity loaded with a  $\text{Bi}_2\text{CuO}_4$  sample grown by the hydrothermal technique at  $\nu=36$  GHz and different temperatures.

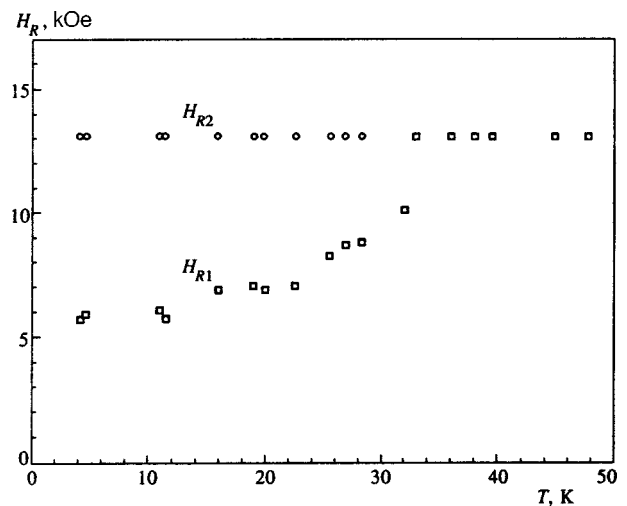


FIG. 7. Resonance fields  $H_{R1}$  and  $H_{R2}$  versus temperature at  $\nu=36$  GHz. The samples were grown by the hydrothermal technique.

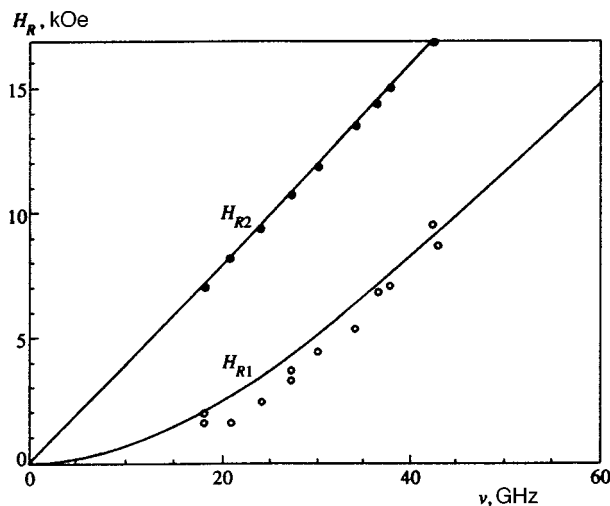


FIG. 8. Resonant fields  $H_{R1}$  and  $H_{R2}$  versus frequency at  $T = 4.2$  K. The samples were grown by the hydrothermal technique.

the line width and intensity in the range of 1.2–25 K are almost independent of the temperature. The amplitude of line  $R2$  rapidly drops with temperature. The resonant fields corresponding to these lines versus frequency are plotted in Fig. 8. At frequencies higher than 45 GHz (i.e., in fields higher than 9–10 kOe) only line  $R2$  can be seen in the spectra. It is highly probable that line  $R2$  is due to paramagnetic defects in the sample, whereas line  $R1$  is caused by excitations in the magnetically ordered crystal. If we assume that the small ferromagnetic moment is caused by the canting of magnetic sublattices due to the Dzyaloshinskii interaction,<sup>9</sup> the Dzyaloshinskii effective field  $H_D$  can be derived from measurements of the resonant field as a function of frequency.<sup>13</sup> The solid curve in Fig. 8 plots a fitting of the resonant field calculated by Eq. (2), where  $H^2$  in the first term on the right-hand side is replaced by  $H(H + H_D)$  and the rest of the constants are the same as in samples grown from a melt. The best fitting was obtained at  $H_D = 20$  kOe. This result is a factor of four larger than the value derived from static measurements of magnetization.<sup>9</sup>

Annealing of crystals grown by the hydrothermal method led to unexpected results. The absorption line  $R1$  vanished after annealing in atmospheres of either oxygen or helium, whereas the position and intensity of line  $R2$  did not change. The annealing was performed under the same conditions as in the case of the crystals grown by the flux method. Given the oxygen deficiency in the initial samples, we expected that annealing in an oxygen atmosphere should have led to the appearance of an AFMR line similar to that of samples grown from a melt, but it was not detected in our experiments. X-ray microanalysis showed that the crystal composition after the annealing in oxygen atmosphere was

$\text{Bi}_{2.05}\text{CuO}_{3.91}$ , i.e., the oxidation degree of cations increased after the annealing, but did not reach the value characteristic to the crystals grown from a melt. It is plausible that the conditions of this annealing are too mild to get rid of the oxygen deficiency in the crystal, but it is sufficient to release local elastic strains in the crystal or make the oxygen concentration uniform over the crystal volume. On the other hand, the difference between the properties of the two types of crystals can be attributed to different ratios between the contents of copper and bismuth.

The elimination of line  $R1$  after annealing in oxygen or helium atmosphere under relatively mild conditions casts doubt on the conjecture about a relationship between the small ferromagnetic moment in  $\text{Bi}_2\text{CuO}_4$  samples manufactured by the hydrothermal technique and canting of sublattices due to the Dzyaloshinskii–Moria interaction. It seems more probable that the resonant absorption in line  $R1$  and the small ferromagnetic moment are due to the presence of domain walls in the samples.

The authors are grateful to L. A. Prozorova, A. I. Smirnov, and S. S. Sosin for fruitful discussions. The work was supported by the Russian Fund for Fundamental Research (Projects 96-02-16575 and 95-02-036-a).

\*E-mail: svistov@kapitza.ras.ru

- <sup>1</sup>H. Ohta, K. Yoshida, T. Matsuya, T. Nanba, M. Motokawa, K. Yamada, Y. Endon, and S. Hosoya, *J. Phys. Soc. Jpn.* **61**, 2921 (1992).
- <sup>2</sup>E. W. Ong, G. H. Kwei, R. A. Robinson, B. L. Ramakrishna, and R. B. von Dreele, *Phys. Rev. B* **42**, 4255 (1990).
- <sup>3</sup>J. C. Boivin, D. Thomas, and G. Tridot, *C. D. Acad. Sci. Paris* **276**, 1105 (1973).
- <sup>4</sup>J. L. Garcia-Muñoz, J. Rodriguez-Carvajal, F. Sapina, M. J. Sanchez, R. Ibañez, and D. Beltran-Porter, *J. Phys. Condens. Matter* **2**, 2205 (1990).
- <sup>5</sup>R. Troc, J. Janicki, I. Filatow, P. Fischer, and A. Murasik, *J. Phys. Condens. Matter* **2**, 6989 (1990).
- <sup>6</sup>K. Yamada, K. Takada, S. Hosoya, Y. Watanabe, Y. Endoh, N. Tomonaga, T. Suzuki, T. Ishigaki, T. Kamiyama, H. Asano, and F. Izumi, *J. Phys. Soc. Jpn.* **60**, 2406 (1991).
- <sup>7</sup>M. Ain, G. Dhahenne, O. Guiselin, B. Hennion, and A. Revcolevschi, *Phys. Rev. B* **47**, 8167 (1992).
- <sup>8</sup>A. I. Pankrats, G. A. Petrakovskii, and K. A. Sablina, *Solid State Commun.* **91**, 121 (1994).
- <sup>9</sup>R. Szymczak, H. Szymczak, A. V. Zalesky, and A. A. Bush, *J. Magn. Magn. Mater.* **140–144**, 1573 (1995).
- <sup>10</sup>G. A. Petrakovskii, K. A. Sablina, A. M. Vorotnikov, V. N. Vasiliev, A. I. Kruglik, A. D. Balaev, D. A. Velikanov, and N. I. Kiselev, *Solid State Commun.* **79**, 317 (1991).
- <sup>11</sup>A. V. Zalesky, V. G. Krivenko, T. A. Khimich, N. E. Ainbinder, and A. A. Bush, *J. Magn. Magn. Mater.* **127**, 281 (1993).
- <sup>12</sup>G. A. Petrakovskii, K. A. Sablina, V. V. Val'kov, and B. V. Fedoseev, A. Furer, P. Fisher, and B. Rossl, *JETP Lett.* **56**, 144 (1992).
- <sup>13</sup>E. A. Turov, *Physical Properties of Magnetically Ordered Crystals* [in Russian], Izd. AN SSSR, Moscow (1963), pp. 61–77.
- <sup>14</sup>J. P. Attfield, *J. Phys. Condens. Matter* **1**, 7045 (1989).
- <sup>15</sup>V. G. Bar'yakhtar and V. L. Sobolev, *Fiz. Tverd. Tela* **15**, 2651 (1973) [*Sov. Phys. Solid State* **15**, 1764 (1973)].

Translation provided by the Russian Editorial office.